The Laryngoscope © 2020 American Laryngological, Rhinological and Otological Society Inc, "The Triological Society" and American Laryngological Association (ALA)

Development of a Bioinspired, Self-Adhering, and Drug-Eluting Laryngotracheal Patch

Solaleh Miar, MS; Gregory R. Dion, MD ; Sergio Montelongo, PhD; Joo L. Ong, PhD; Rena Bizios, PhD; Teja Guda, PhD

Objectives/Hypothesis: Novel laryngotracheal wound coverage devices are limited by complex anatomy, smooth surfaces, and dynamic pressure changes and airflow during breathing. We hypothesize that a bioinspired mucoadhesive patch mimicking how geckos climb smooth surfaces will permit sutureless wound coverage and also allow drug delivery.

Study Design: ex-vivo.

Methods: Polycaprolactone (PCL) fibers were electrospun onto a substrate and polyethylene glycol (PEG) – acrylate flocks in varying densities were deposited to create a composite patch. Sample topography was assessed with laser profilometry, material stiffness with biaxial mechanical testing, and mucoadhesive testing determined cohesive material failure on porcine tracheal tissue. Degradation rate was measured over 21 days in vitro along with dexamethasone drug release profiles. Material handleability was evaluated via suture retention and in cadaveric larynges.

Results: Increased flocking density was inversely related to cohesive failure in mucoadhesive testing, with a flocking density of PCL-PEG-2XFLK increasing failure strength to 6880 ± 1810 Pa compared to 3028 ± 791 in PCL-PEG-4XFLK density and 1182 ± 262 in PCL-PEG-6XFLK density. The PCL-PEG-2XFLK specimens had a higher failure strength than PCL alone (1404 ± 545 Pa) or PCL-PEG (2732 ± 840). Flocking progressively reduced composite stiffness from 1347 ± 15 to 763 ± 21 N/m. Degradation increased from 12% at 7 days to 16% after 10 days and 20% after 21 days. Cumulative dexamethasone release at 0.4 mg/cm² concentration was maintained over 21 days. Optimized PCL-PEG-2XFLK density flocked patches were easy to maneuver endoscopically in larvngeal evaluation.

Conclusions: This novel, sutureless, patch is a mucoadhesive platform suitable to laryngeal and tracheal anatomy with drug delivery capability.

Key Words: Laryngeal patch, mucoadhesive, drug delivery, repair, closure.

Level of Evidence: N/A

Laryngoscope, 00:1-9, 2020

INTRODUCTION

Esophageal and laryngotracheal wound closure is complicated by unique three-dimensional anatomy, exposure to commensal organisms, presence of mucus and secretions, and the overarching need for achieving an airand

From the Department of Biomedical Engineering (S.M., G.R.D., S.M., J. L.O., R.B., T.G.), University of Texas at San Antonio, San Antonio, Texas, U. S.A.; Dental and Craniofacial Trauma Research Department (G.R.D.), U.S. Army Institute of Surgical Research, San Antonio, Texas, U.S.A.

Editor's Note: This Manuscript was accepted for publication on September 19, 2020

Funding for the work described in this manuscript was provided, in part, by the National Science Foundation Award (CBET#1847103; Principal Investigator-Guda) and the San Antonio Area Foundation (Principal Investigator-Guda).

The authors have no other funding, financial relationships, or conflicts of interest to disclose.

This manuscript was submitted for presentation at the American Laryngological Association Annual Meeting at the Combined Otolaryngology Spring Meetings in Atlanta, GA, April 22-26, 2020.

The views expressed in this manuscript are those of the authors and do not reflect the official policy or position of the Department of the Army, Department of the Air Force, Department of Defense, or the US Government.

Send correspondence to Gregory R. Dion, MD, MS, Dental and Craniofacial Trauma Research Department, U.S. Army Institute of Surgical Research, 3698 Chambers Pass, Bldg 3611, JBSA Fort Sam Houston, San Antonio, TX 78234. E-mail: gregory.r.dion.mil@mail.mil

DOI: 10.1002/lary.29182

Laryngoscope 00: 2020

water-tight closure. Furthermore, the healing trachea and esophagus must remain functional in the absence of a tracheostomy or percutaneous endoscopic gastrostomy tube. Penetrating wounds to the larynx, trachea, and esophagus most often occur during surgical intervention or from trauma. Recent evaluation identified acute laryngeal injury in more than half of patients intubated >12 hours, with findings persisting for >2 months.¹ Although less common, esophageal injuries from caustic ingestion are a significant health burden in the pediatric population, and esophageal perforations demonstrate significant morbidity.^{2, 3} Inadequate wound closure results in serious complications including pneumomediastinum, deep neck space infection, or mediastinitis. 4-6 Currently, the most widely used closure techniques are primary closure and overlay with adjacent muscle tissue. Evidence suggests that early intervention may be ideal for treating patients, because few effective alternatives exist.

Adjuvant closure techniques for esophageal and laryngotracheal wounds include salivary bypass tubes, stents, and skin grafting. 9-13 These have had mixed success and are limited by associated morbidity from salivary bypass tubes or secondary harvest sites and subsequent skin graft changes which may still not provide air- or water-tight closure. 9, 11 In addition, few available stents are capable of delivering therapeutics.

Application of biomaterial and tissue-engineered products holds promise as evidenced by preliminary data using connective tissue-based biosheets for esophagoplasty.¹⁴

Recent advances in biomimetic materials provide unique opportunities for new technology targeting unmet clinical needs. Specifically, recent work leveraging the mechanism geckos and mussels use to attach to wet, irregular surfaces holds promise in inspiring materials designed for adhesion in moist environments. ^{15, 16} These new materials are manufactured by adapting flocking technology from the textile industry whereby short, vertical fibers are affixed to a base layer to design the composite construct. ¹⁷ These composites can potentially provide improved, reversible adhesion compared to traditional bio-polymers. ^{18, 19} Originally envisioned as adhesive tapes or as stability mechanisms in robotic climbers, they can also function as scaffolds in tissue engineering. ²⁰

The design of a base layer for tissue sealants requires materials capable of conforming to the gross that control fluid permeability maintaining biocompatibility. Electrospinning is the preferred technique for creating fibrous mats in controlled. designed architectures. Electrospun fibers are manufactured by applying high voltage between a nozzle and collector to create a polymer stream, and can be optimized for desired fiber diameter, orientation, and mat thickness.²¹ A variety of polymers can be electrospun for biomedical applications.^{21–23} Polycaprolactone (PCL), a biocompatible polymer is of specific interest for tissue engineering because it presents low inflammatory response,²⁴ especially when used as electrospun fibers.^{24, 25} In addition, electrospinning lends itself well to incorporating drugs within the fibers, providing novel drug delivery approaches.^{23, 26, 27} In a preclinical guinea pig model, vancomycin-embedded electrospun coatings on middle ear prostheses reduced methicillin resistant Staphylococcus aureus biofilm formation.²⁸ Particularly relevant to applications in the laryngotracheal complex, dexamethasone incorporation into electrospun PCL has shown encouraging immunomodulation in vitro and ex vivo. $^{29-31}$

Collectively, the capability of flocking to mimic the gecko's adhesive ability and concomitant drug delivery from both the flocks and electrospun fibers lays the framework for a technology platform with tremendous translational potential. In this study, we hypothesized that by leveraging flocking and electrospinning, it would be possible to create a flexible, mucoadhesive patch capable of drug delivery for further use in the esophagus and laryngotracheal complex.

MATERIALS AND METHODS

Synthesis of Adhesive Patches

To fabricate dexamethasone-loaded polycaprolactone (PCL) electrospun fibers, PCL pellets (M_W : 80,000) were dissolved in chloroform and ethanol (15:85 v/v) and dexamethasone (1:10 Dexamethasone:PCL w/w) was added. Final solutions were electrospun at a traveling distance 30 cm, flow rate 1.4 ml/hr, and applied voltage of 25 KV.

Fiber mats created were soaked in 4-arm Polyethylene Glycol Acrylate (4APEGA, M_W:20,000, JenKem Technology, Plano,

TX) dissolved in deionized water containing 0.1% 2-Hydroxy-4′-(2-hydroxyethoxy)-2-methylpropiophenone (Sigma-Aldrich, St. Louis, MO) in ethanol for 15 minutes to create an adhesive coating for flock attachment. Samples were then centrifuged (15 seconds at 500 rpm) to remove excess 4APEG.

Coated fiber substrates were placed in the flocking system 5 cm from sieved 4APEGA stock, and various voltages (1, 2, 4, and 6 KV/cm) were applied to produce different flocking concentrations. The applied voltage forces flock particles to propel toward the fiber substrate.^{33, 34} Postdeposition, samples were exposed to UV light for 5 minutes to permanently bond flocks to the surface by crosslinking. Samples were re-immersed in dexamethasone (10 mg/ml), to load flocks with the drug. Table I lists the experimental groups. All chemicals were purchased from Thermofisher (Waltham, MA) unless otherwise specified.

Topographical Characterization

A Keyence VK-X200 laser microscope was used for threedimensional profiling to quantify flock structure, height, and dispersion. Each specimen was mounted on a glass slide, a nine-quadrant grid was assigned around the specimen center (20× magnification), and upper and lower focus limits for the surface were set. Profilometry data were collected using VK Viewer software (v2.5, Keyence Corp., Osaka, Japan), imported into the multifile analyzer (v1.1.22.87, Keyence Corp.) and surface roughness, line roughness, and multiline roughness were computed for each sample (n = 6/group).

Mechanical Property Characterization

Biaxial mechanical testing was conducted on biomaterial patches and on the inner layer of fresh porcine trachea using the BioTester (CellScale Biomaterials Testing, Ontario, Canada). ³⁵ 1.5 cm square specimens (n = 10/group, n = 30/trachea) were equilibrated in phosphate buffered saline (PBS) at room temperature. Specimen were held by rakes and stretched to 10% strain equibiaxially. The stress versus strain graphs for each direction were approximated by a sixth order polynomial using MATLAB_R2020A and the slope of the tangent line was calculated at 20% strain using the derivative of the polynomial to determine elastic modulus.

Swelling and Degradation Studies

One centimeter square samples (n = 6/group) were weighed before the experiment and placed in PBS buffer at $37^{\circ}\mathrm{C}.$

TABLE I.
The Description of Designed Groups and Electro-Flocking
Parameters.

Group	Structure Description	Electroflocking Electric Field
PCL	PCL electrospun fibers only	N/A
PCL-PEG	PCL electrospun fibers coated with 4APEGA	N/A
PCL-PEG-FLK	Flocked 4APEGA coated PCL fibers	1 KV/cm
PCL-PEG-2XFLK	Flocked 4APEGA coated PCL fibers	2 KV/cm
PCL-PEG-4XFLK	Flocked 4APEGA coated PCL fibers	4 KV/cm
PCL-PEG-6XFLK	Flocked 4APEGA coated PCL fibers	6 KV/cm

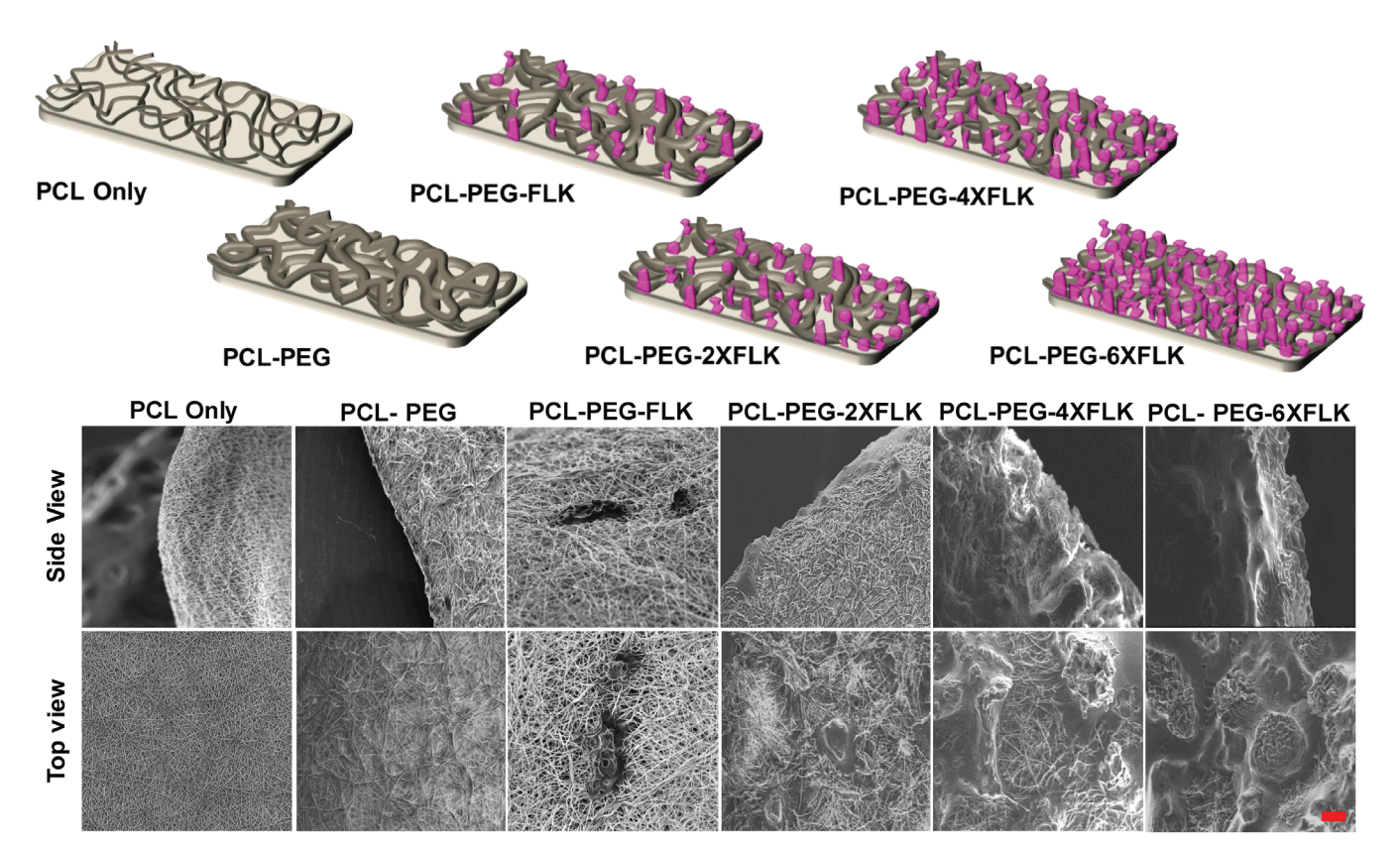


Fig. 1. Schematic representation and scanning electron micrography of the six patch designs developed. The base electrospun PCL fiber patch was coated in PEG to form the PCL-PEG substratum. Upon this substratum, flocking was performed to add 4 increasing densities of PEG flocks, which were then labelled PCL-PEG-FLK, PCL-PEG-2XFLK, PCL-PEG-4XFLK and PCL-PEG-6XFLK to denote increasing relative concentration of surface flocks. Scanning Electron Microscopy was conducted on coated dry samples under 20 KV and micrographs are presented from top and side views. The scale bar represents 100 μm. [Color figure can be viewed in the online issue, which is available at www. laryngoscope.com.]

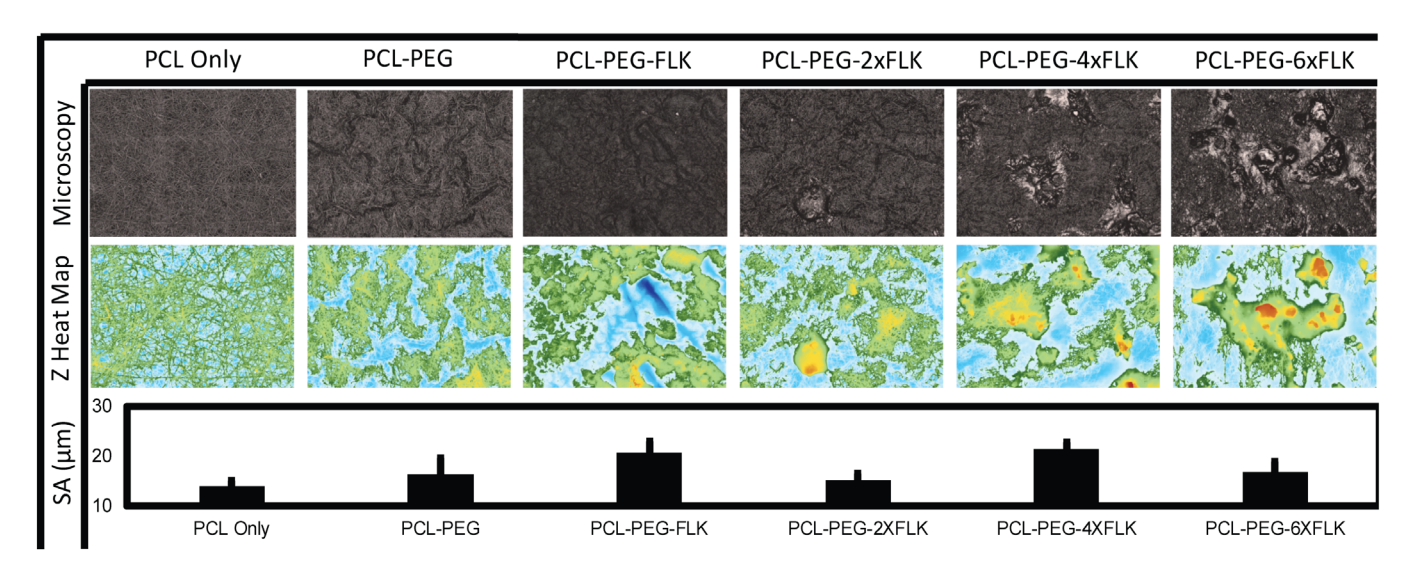


Fig. 2. Laser Profilometry to measure surface features. (A) Microscopy images of the 2 mm \times 1.5 mm rectangular areas visualized in the optical scan. (B) Heat maps generated from the laser profilometry showing high peaks in red and base substrate in deep blue. (C) Surface arithmetical mean height (SA) measured for each group (n = 6). SA shows the difference between the heights of each point compared to the arithmetical mean of the samples' surface. According to the results, the data showed no significant SA results. [Color figure can be viewed in the online issue, which is available at www.laryngoscope.com.]

Swelling ratio was measured every 5 minutes by recording weight gain after removing excess PBS until swelling equilibrium (at 30 minutes). The degradation mass loss was recorded weekly over 21 days. The swelling or degradation ratio was calculated as $(M_f - M_i)/(M_i)$, where M_i and M_f are the mass of samples in its initial and final states, respectively.

Mucoadhesion Testing

Mucoadhesion was measured in single lap shear mode (using standard ASTM F2255) using a U-Stretch machine (CellScale Biomaterials Testing, Ontario, Canada). Samples (n = 6/group) hydrated with PBS were cut 1 cm square strips and adhered to fresh porcine trachea. The adhesive joint was held compressed for 2 hours under 100 grams weight. Samples were then loaded to failure at 10 mm/min, and the cohesion strength was measured.

Drug release behavior

Dexamethasone release from the drug-loaded PCL fibers, PCL-PEG, and samples with different flock concentrations was

studied over 28 days (n = 6/group) in PBS buffer at 37°C. To study burst release, the early release was measured after 15, 30, 60, and 120 minutes and to study sustained release, measurements were performed every 4 days over 28 days. Absorbance of dexamethasone at 290 nm³⁶ was measured using a plate reader and reported as mass/cm².

Suturability Testing

Suture retention strength was measured using the UStrech machine using an adapted AAMI protocol. $^{37-40}$ Briefly, samples (n = 6/group) were cut into 12×5 mm and polyglycolic acid 4/0 sutures were looped through each sample 2 mm from the free end. A ramp-to-failure test was executed at 10 mm/min until tear-out. The suture retention failure strength was normalized to sample thickness.

Cadaveric Material Testing

To determine patch handleability, realistic adhesion, and application in vivo, fresh frozen cadaveric larynges were thawed

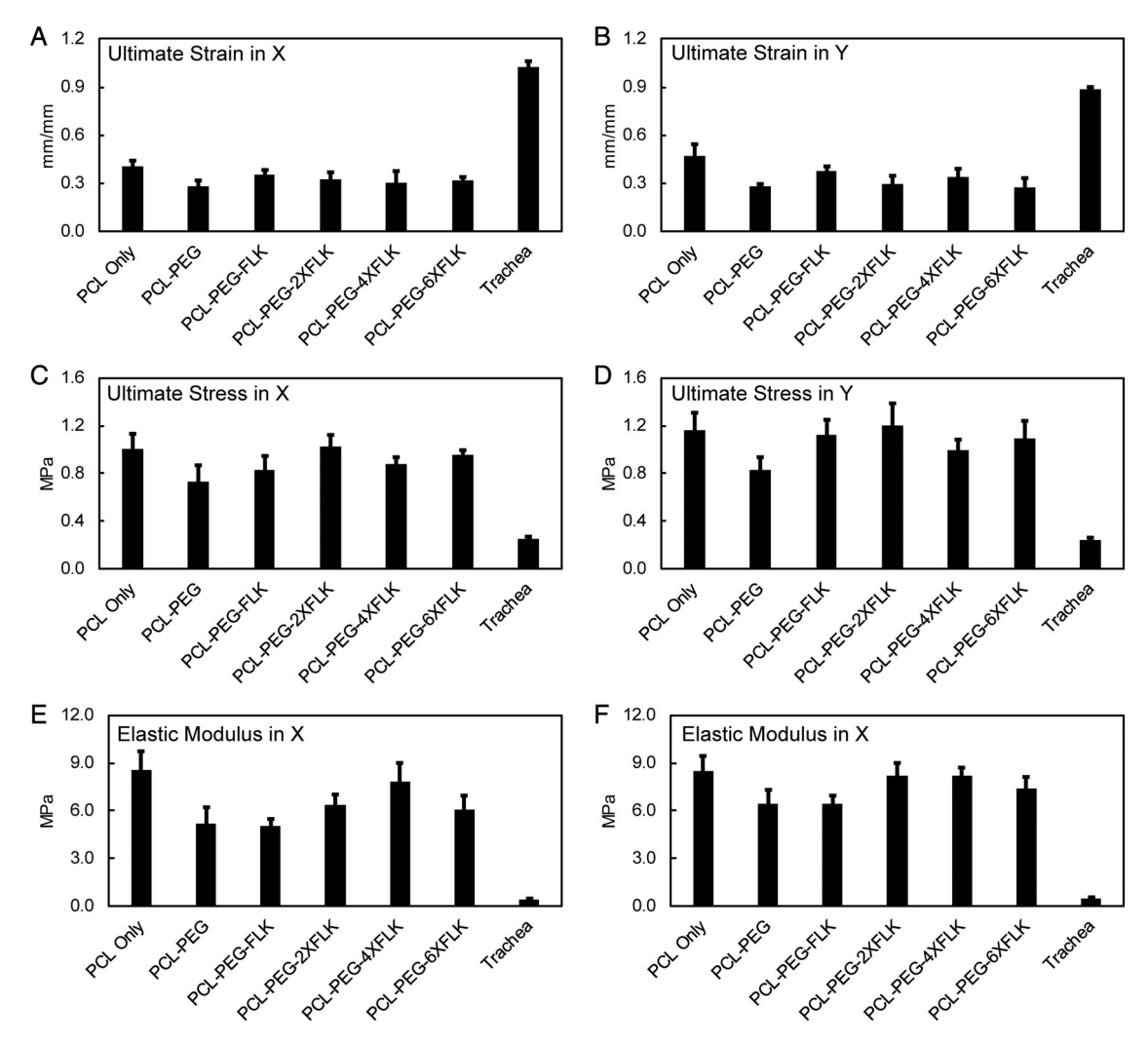


Fig. 3. Biaxial mechanical testing. The 6 different materials and native porcine tracheal tissue were tested in biaxial extension to failure and ultimate strain at failure in the (A) X and (B) Y direction, ultimate stress at failure in the (C) X and (D) Y direction and elastic modulus of the tissue in the (E) X and (F) Y direction were calculated. Tracheal properties were distinctly different from all other materials tested for all parameters (P < .001), whereas there were no significant differences in material mechanics between the groups themselves, except that the PCL-PEG and PCL-PEG-FLK group had significantly lower elastic modulus than the PCL Only group (P = .05).

to room temperature and placed in a hollow PVC pipe below a microscope to replicate microlaryngoscopy. Patches were trimmed to 1×2 cm for simulated use, hydrated in saline (n = 6 technical replicates). Using a 400 mm microscope and microlaryngeal graspers, samples were passed into the larynx, overlaid on the vocal folds, and then removed and pressed against the anterior wall of the subglottic and trachea. Material tears or pliability restrictions limiting maneuverability or positioning and the ability or lack of attachment to the mucosal lining were noted. All simulations were performed by a fellowship trained laryngologist.

Statistical Analyses

Numerical data are reported as average \pm standard error. Significant differences (at P < .05) were identified using one-way Analysis of Variance (ANOVA), followed by Tukey's post hoc test, using SigmaPlot (v13, Systat Software Inc, San Jose, CA).

RESULTS

Scanning electron microscopy (SEM) demonstrated successful PCL electrospinning, uniform 4APEGA coating in the PCL-PEG group, and flock attachment to the substrate in PCL-PEG-FLK, PCL-PEG-2XFLK, PCL-PEG-4XFLK, and PCL-PEG-6XFLK groups. Less homogeneity of flocks were observed in PCL-PEG-FLK whereas flock concentration increased in PCL-PEG-2FLK and PCL-PEG-4XFLK groups where distinct flocks were visualized, and in the PCL-PEG-6XFLK group the flocks were increasingly aggregated (Fig. 1). The side profile view indicated an increase in flock height in groups with higher flock concentration. of large local clusters of 4APEGA flocks (Fig. 1).

Roughness measurements varied amongst the groups, visualized via Z heat maps, and quantified by surface arithmetical (SA) mean height (Fig. 2A–C). The Z heat maps (Fig. 2B), supported SEM observations, that

flock height increased with flock concentration (deep blue and deep red represent the lowest valleys and highest peaks, respectively). It was observed that changes in SA (measured in μm); the difference between point heights compared to mean sample surface level did not correlate to applied voltage and consequently to flock concentration. Although SA measurements were not significantly different, the highest SA values were recorded in the PCL-PEG-FLK (21 \pm 2.3 μm) and PCL-PEG-4XFLK (21.4 \pm 1.4 μm) groups whereas the lowest SA value was recorded for PCL (14.1 \pm 0.9 μm). The relatively lower SA of the PCL-PEG-6XFLK group (17.0 \pm 2.1 μm) quantitatively supports flock clusters forming on the substrate resulting in increased average surface height, but a decrease in calculated surface roughness.

Biaxial mechanical behavior measurements indicated minor numerical differences, but no difference in trends between groups for any metric between longitudinal and circumferential directions (Fig. 3). Elastic modulus (P < .0001) and ultimate stress (P = .0001) were significantly lower and ultimate strain was significantly higher (P < .0001) in the native tracheal membrane, than all tested groups. Because the patches were designed to be homogenous, no differences were observed in mechanical properties along the two directions as anticipated. Further, no significant differences were measured in properties due to the coating or flocks.

Burst release over the first 2 hours and sustained dexamethasone release over 28 days was observed for all groups tested. A controlled burst release of dexamethasone was observed in the PCL-PEG-FLK, PCL-PEG-2XFLK, PCL-PEG-4XFLK, and PCL-PEG-6XFLK groups (Fig. 4A) over the first 2 hours which is associated with the presence of 4APEGA either in the coating or the flocks and the burst release correlated with flock concentration. Over 28 days (Fig. 4B), the remaining drug was associated with dexamethasone incorporated in PCL

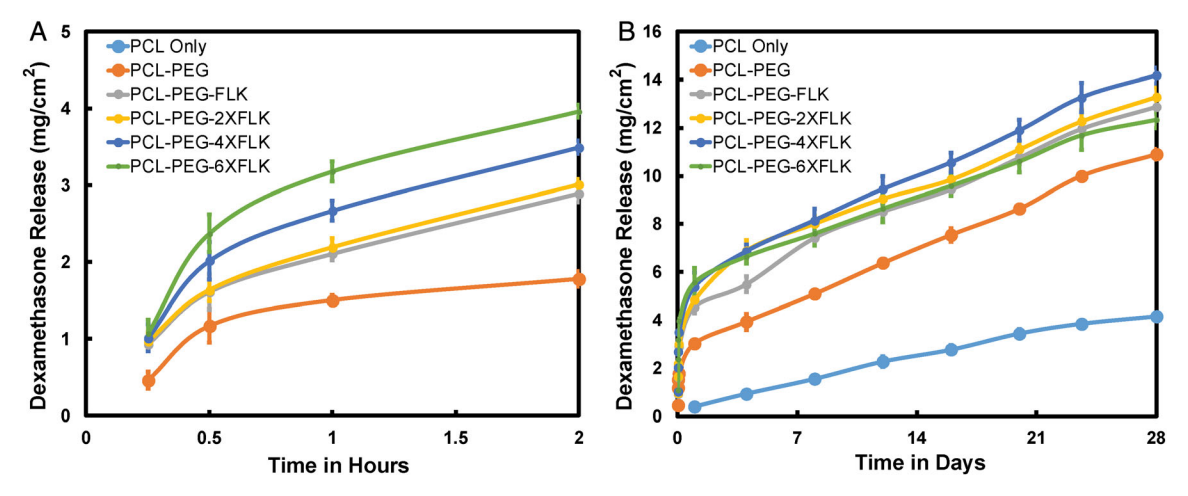


Fig. 4. Dexamethasone release from the patches over 28 days. Dexamethasone release was measured for each group (A) every half hour over the first 2 hours, to evaluate burst release behavior and (B) then at days 1, day 4 and every 4 days to day 28 to evaluate sustained release. No measurable release was observed from the PCL Only group over the first 2 hours, and no significant difference were found between these groups over the 2 hour burst release period. At Days 4 and 8, the PCL-PEG-2XFLK, PCL-PEG-4XFLK and PCL-PEG-6XFLK showed significantly greater release than the PCL Only and PCL-PEG groups (P < .001), at days 12 and 16, the PCL only group showed significantly lower release than all FLK groups (P < .001), and at days 20, 24 and 28, the PCL only group showed significantly lower release than all other groups (P < .001). [Color figure can be viewed in the online issue, which is available at www.laryngoscope.com.]

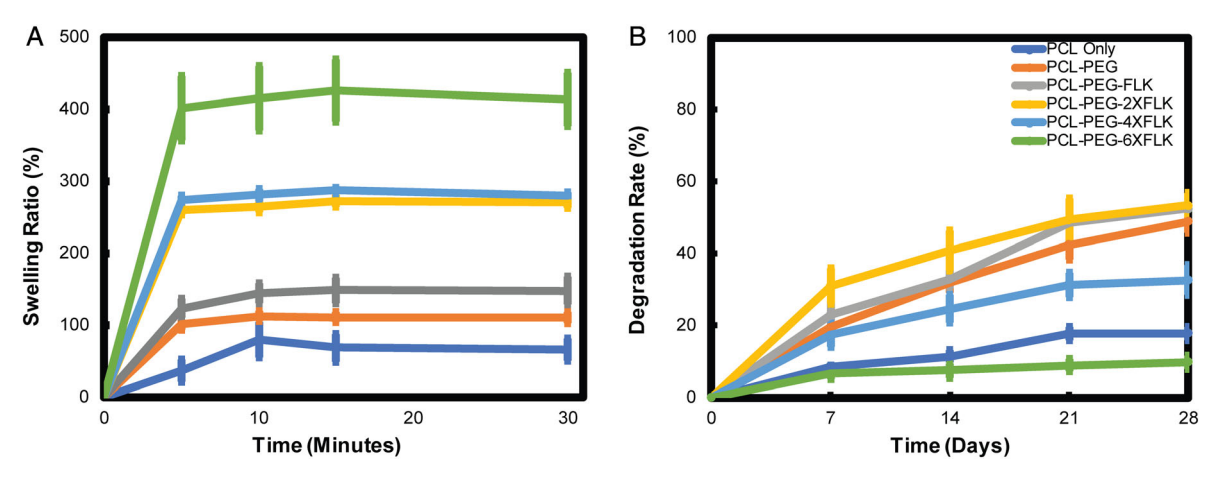


Fig. 5. (A) Swelling behavior. Swelling ratio of patches in PBS (at room temperature) over time. The water absorbency was measured every 5 minutes until the samples reached the swelling equilibrium. (B) Material degradation over time. Material degradation of each group was measured over a 28 day period and all groups stabilized after the initial degradation within the first 7 days, such that there was a main effect of the 21 and 28 day time points being significantly different from the 0 and 7 day time points across all groups (*P* < .05). Degradation was significantly lower in the PCL only and PCL-PEG-6XFLK groups compared to other groups, such that their degradation was significantly lower compared to the PCL-PEG-FLK and PCL-PEG-2XFLK groups for all time points day 7 and later, and compared to all other groups at day 14 and later (*P* < .03). [Color figure can be viewed in the online issue, which is available at www.laryngoscope.com.]

fibers and a sustained release was observed across all groups. The PCL fiber mat demonstrated the lowest drug release (~ 4 mg/cm²), whereas the 4APEGA coated and flocked patches released ~ 14 mg/cm² of dexamethasone over 28 days.

Swelling ratio is crucial to drug release behavior because diffusion of water into the 4APEGA network leads to dexamethasone dissolution. In addition, mucoadhesion forces must overcome the swollen weight of the adhesive patch to ensure it remains in place, making it a crucial deisgn consideration. The groups tested reached swelling equilibrium after 15 minutes, further explaining diffusion-based burst release behavior (Fig. 5A). The highest degradation was observed in the PCL-PEG ($48.8\pm3.1\%$), PCL-PEG-FLK ($52.4\pm1.5\%$), and PCL-PEG-2XFLK ($53.4\pm3.5\%$) groups whereas degradation was significantly lower in PCL only($17.8\pm1.8\%$) and PCL-PEG-6XFLK ($9.8\pm1.8\%$) groups (Fig. 5B). Specifically, the degradation in PCL and PCL-PEG-6XFLK groups was significantly lower than in PCL-PEG-FLK and PCL-PEG-2XFLK groups for all time points day seven and later, and lower compared to PCL-PEG at day

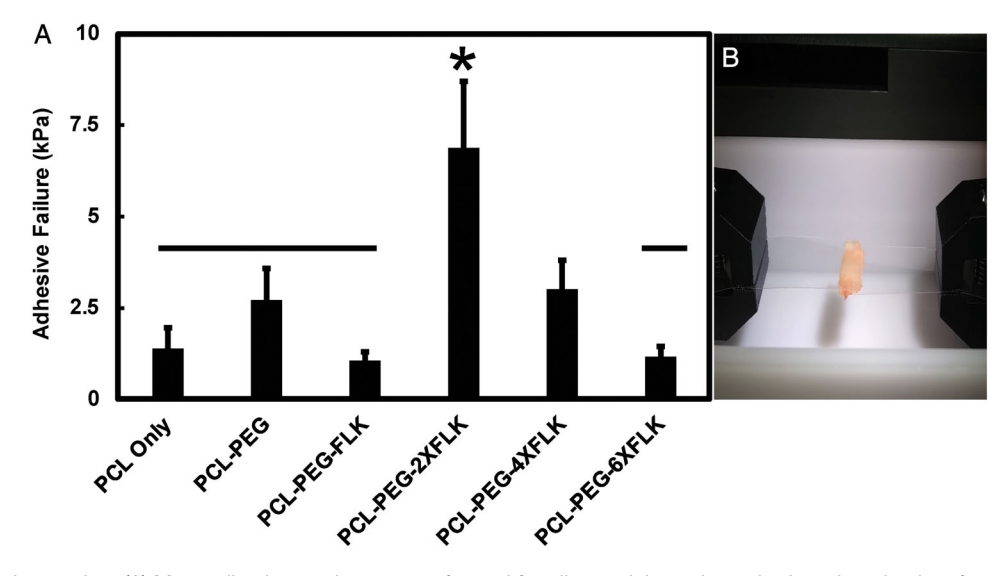


Fig. 6. Mucoadhesion testing. (A) Mucoadhesion testing was performed for all materials against a hydrated tracheal surface with intact mucosa in lap shear mode. It was found that the PCL-PEG-2XFLK group demonstrated significantly greater (* indicates significantly different at P < .05) stress at adhesive failure compared to all groups except PCL-PEG-4XFLK (different from PCL-PEG-4XFLK at P = .09). (B) Mucoadhesion experiment on fresh porcine trachea conducted using single lap shear protocol. Patches were connected to fixturing on the UStretch machine and the trachea specimens were attached to the actuator. The experiment was conducted at a strain rate of 10 mm/min. [Color figure can be viewed in the online issue, which is available at www.laryngoscope.com.]

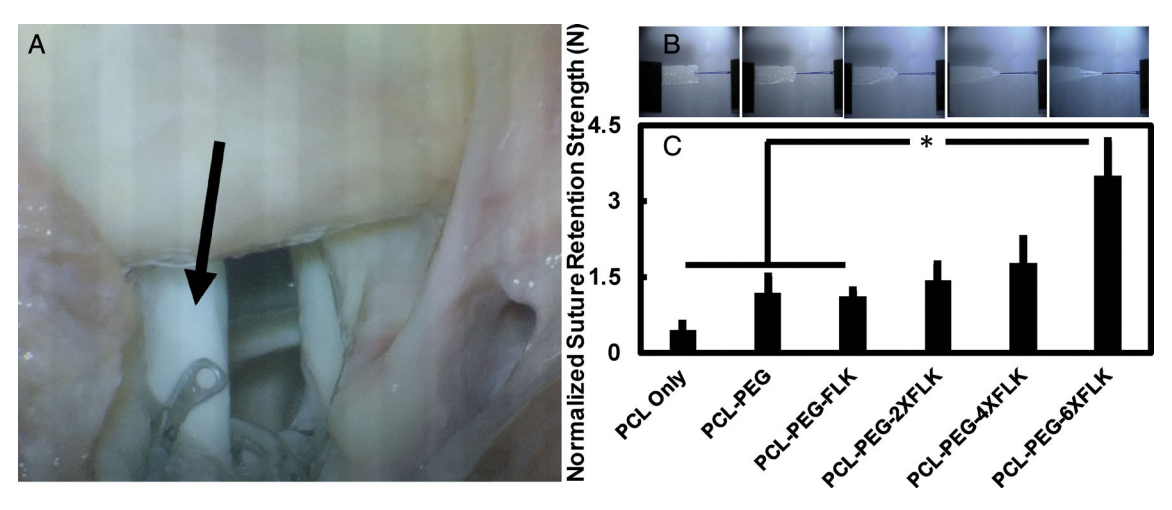


Fig. 7. (A) In situ adhesion in a cadaver model and suturability properties. In-procedure imaging of the prepared flocked patch (PCL-PEG-2XFLK) adhering to the vocal fold area of the larynx. (B) Top views of patch failure in suture retention experiment. Circumferential tearing pattern and crack propagation were observed during progression of the test, to breakage. (C) Suture retention strength. Failure strength of the suture measured in the PCL-PEG-6XFLK was significantly higher than PCL only, PCL-PEG, PCL-PEG-FLK (P < .025). [Color figure can be viewed in the online issue, which is available at www.laryngoscope.com.]

14 and later (P < .03). 4APEGA is known to have low degradation rate due to high molecular weight⁴¹; and therefore, agglomeration of flocks resulted in a more stable structure resistant to flock detachment whereas in other groups with more dispersed flocks, detachment resulted in higher mass loss (Fig. 5B).

The highest mucoadhesive strength was observed in the PCL-PEG-2XFLK group (6879 Pa), and the lowest adhesion was observed for PCL-PEG (1053 Pa) (Fig. 6). PCL-PEG-2XFLK patches showed significantly higher adhesion to mucosa compared to PCL alone, PCL-PEG, PCL-PEG-FLK, and PCL-PEG-6XFLK (P=.004, .042, .002, and .004, respectively) but not PCL-PEG-4XFLK flocking (P=.092).

Sample testing in simulated microlaryngoscopy cases revealed pliable, easily handled, and manipulated patches (Fig. 7A). Patches were found to adhere to the subglottic/trachea mucosa but also allowed for adjustment/manipulation for position optimization. Figure 7B illustrates tear-out failure resistance in suture retention of the engineered patches. The lowest suture retention strength was recorded in PCL $(0.45 \pm 0.13 \text{ N})$ and an increasing trend was observed with increasing flock concertation, the highest suture retention strength was measured for PCL-PEG-6XFLK $(3.5 \pm 0.7 \text{ N})$ (Fig. 7C). Suture retention strength in PCL-PEG-6XFLK was significantly higher than in PCL PCL-PEG, and PCL-PEG-FLK groups (P = .001, .022, and .023 respectively).

DISCUSSION

Translational implementation of novel materials and therapeutic delivery systems is needed for the management of laryngotracheal and esophageal wounds. Medical adjuncts such as steroids, antibiotics, and anti-inflammatory medications have been studied clinically, but an urgent need for efficient delivery approaches remains. 42, 43 Intralesional and in-office steroid injection

remain current best practice for subglottic and tracheal stenosis.44-46 These interventions appear to reduce disease progression and increase interval between repeat procedures. Despite compelling evidence for their effectiveness, application of corticosteroids to the stenotic region remains limited by practical considerations of performing in-office injection involving flexible videolaryngoscopy and transcutaneous injection. 46 Leveraging our novel patch allows for continuous drug delivery across the desired surface, filling an unmet clinical need. In addition to expanding the possible dose and durations for steroid treatment, this approach could reduce currently necessary injections. Similarly, few effective adjuvant therapies are available for glottic webs beyond keels and stents. 47 Interest in improved management of webs is evidenced by recent studys exploring bovine pericardium as a potential graft material and advanced surgical closure techniques. 48, 49 Our novel patch could fill this role and be used with or without accompanying drug delivery.

Topography and surface contact area play a large role in final adhesive forces. ¹⁹ Hydrogel based adhesives demonstrate enhancement via interlocking mechanisms activated by swelling of PEG components. 50 Surface roughness is critical to mucoadhesive properties $^{19,\ 50}$ and mucosa-material interaction is multifactorial, with contributions from moisture, surface roughness, and surface area/shape. The gecko's ability to adhere to surfaces using setae on its feet, involves factors including water contact angle, Van der Waals forces, capillary forces, and geometry.⁵¹ In our study, both roughness and surface contact area varied with flock density (Figs. 1 and 2). Differences in roughness and inherent to varying patch designs in our study allowed for optimal design selection in terms of surface flock density. A very low density of flocks on the patch resulted in low adhesive force to tracheal mucosa which first increased and then decreased at higher surface flocking densities (Fig. 6). Furthermore, preload plays a crucial role in the ultimate adhesive properties.

In our evaluation, all samples had equivalent preload force and duration prior to quantification. The improved cohesive adhesion of PCL-PEG-2XFLK in our study can be attributed to an optimized flock concentration leading to mechanical interlocking between the flocks and mucin layer of the tracheal wall. Conversely, the PCL-PEG-4XFLK and PCL-PEG-6XFLK groups have higher flock concentrations, and the lower adhesion properties in these groups could be related to decreased available area for adhered surface-flock interaction.

The adhesive properties of the patch are particularly critical in the moist environment of the trachea and esophagus. Sufficient mucoadhesion is also necessary for efficient and optimized drug delivery. 52, 53 To date, an effective route of predictable corticosteroid delivery to local tissue remains elusive. In the nasal cavity, dexamethasone stents showed promise in modulating wound healing.⁵⁴ Our novel flocked patch effectively delivered a sustained release of corticosteroid over 28 days while also providing an initial burst release. The initial burst observed during the first 2 hours was related to the higher PEG volume of flocks. Also, the presence of flocks caused greater drug release compared to PCL-PEG, underlining the impact of flocks on the uptake and release of dexamethasone. Jointly, the adhesive properties prevent unintentional dislodgement, but postrelease flock degradation permits removal for follow-up evaluations or at the conclusion of planned treatment.

Although different implant-based drug delivery approaches have been developed for otorhinolaryngology applications, ⁴³ less attention has been paid to handleability, suturability, and general mechanical suitability. Mechanical forces play a prominent role in fibrosis through T-cell mediated prolonged inflammation. ⁵⁵ Modified interfaces with highly adhesive surfaces and reinforced mechanical properties provide a customizable therapeutic platform which can benefit laryngotracheal wound treatments. Although mechanical properties of the patches are comparable to native tissue, the specific impact of differential mechanical stiffness on fibroblast recruitment and epithelialization requires further study.

Critically, the study was limited to in vitro, ex vivo. and cadaveric testing. The degradation and drug delivery tests were conducted over 28 days, because practically, most nonbioresorbable patches, stents, keels, and glottic webs are typically removed 10 to 14 days after placement. Materials used in our patch match those currently used without cytotoxicity in other FDA approved devices, and can be further assessed in future preclinical in vivo tests. Mucoadhesion testing was performed on excised porcine trachea with reproducible preload force. However, the tracheal microenvironment in vivo varies from the ex vivo counterpart with increased local temperature, mucocilliary function, and a distinct local microbiome which may confer additional adhesion based on flocking; though in vivo studies are needed to quantify differences. The capacity of the flocked patch to remain secure to the laryngotracheal complex without unintentional sloughing can also better be assessed in future in vivo studies. Similarly, outside of intranasal dexamethasone stent evaluation, optimal concentration for continuous steroidal

delivery to laryngotracheal wounds remains unknown. Despite these limitations, the in vitro, ex vivo and cadaveric testing of the self-adhering patch permitted design optimization and preparation for preclinical testing toward clinical application.

CONCLUSION

This novel, sutureless, patch is a mucoadhesive platform suitable to laryngotracheal anatomy with drug delivery capability. Preliminary testing supports the translational potential of this technology for further preclinical evaluation.

ACKNOWLEDGMENT

This research was supported in part by the Presidential Distinguished Research Fellowship to SM, the National Science Foundation CAREER Award (CBET#1847103) and a San Antonio Area Foundation award to TG, funds from the Lutcher Brown Endowment to RB, and the USAA Foundation Endowment to JLO.

BIBLIOGRAPHY

- Shinn JR, Kimura KS, Campbell BR, et al. Incidence and outcomes of acute laryngeal injury after prolonged mechanical ventilation. Crit Care Med 2019:47:1699–1706
- Sdralis EIK, Petousis S, Rashid F, Lorenzi B, Charalabopoulos A. Epidemiology, diagnosis, and management of esophageal perforations: systematic review. Dis Esophagus 2017:30:1-6.
- Hoffman RS, Burns MM, Gosselin S. Ingestion of caustic substances. N Engl J Med 2020;382:1739–1748.
- DeMers G, Camp JL, Bennett D. Pneumomediastinum caused by isolated oral-facial trauma. Am J Emerg Med 2011;29:841.e843–841.e848.
- Velhonoja J, Lääveri M, Soukka T, Irjala H, Kinnunen I. Deep neck space infections: an upward trend and changing characteristics. Eur Arch Otorhinolaryngol 2020;277:863–872.
- Yu AW, Rippel RA, Smock E, Jarral OA. In patients with post-sternotomy mediastinitis is vacuum-assisted closure superior to conventional therapy? *Interact Cardiovasc Thorac Surg* 2013;17:861–866.
- Huu Vinh V, Viet Dang Quang N, Van Khoi N. Surgical management of esophageal perforation: role of primary closure. Asian Cardiovasc Thorac Ann 2019;27:192–198.
- Nouraei SA, Singh A, Patel A, Ferguson C, Howard DJ, Sandhu GS. Early endoscopic treatment of acute inflammatory airway lesions improves the outcome of postintubation airway stenosis. *Laryngoscope* 2006;116: 1417–1421.
- Nouraei SA, Sandhu GS. Outcome of a multimodality approach to the management of idiopathic subglottic stenosis. Laryngoscope 2013;123: 2474–2484.
- Bowe SN, Wentland CJ, Sandhu GS, Hartnick CJ. Management of complex pediatric laryngotracheal stenosis with skin graft reconstruction. Int J Pediatr Otorhinolaryngol 2018;108:46–48.
- Kim AW, Liptay MJ, Snow N, Donahue P, Warren WH. Utility of silicone esophageal bypass stents in the management of delayed complex esophageal disruptions. Ann Thorac Surg 2008;85:1962–1967.
- Chen S, Shapira-Galitz Y, Garber D, Amin MR. Management of Iatrogenic Cervical Esophageal Perforations: a narrative review. JAMA Otolaryngol Head Neck Surg 2020;146:488.
- Moonsamy P, Sachdeva UM, Morse CR. Management of laryngotracheal trauma. Ann Cardiothorac Surg 2018;7:210–216.
- Okuyama H, Umeda S, Takama Y, Terasawa T, Nakayama Y. Patch esophagoplasty using an in-body-tissue-engineered collagenous connective tissue membrane. J Pediatr Surg 2018;53:223–226.
- Lee H, Lee BP, Messersmith PB. A reversible wet/dry adhesive inspired by mussels and geckos. Nature 2007;448:338–341.
- Menguc Y, Rohrig M, Abusomwan U, Holscher H, Sitti M. Staying sticky: contact self-cleaning of gecko-inspired adhesives. J R Soc Interface 2014; 11:20131205.
- 17. Walther A, Bernhardt A, Pompe W, et al. Development of novel scaffolds for tissue engineering by flock technology. $Text\ Res\ J\ 2007;77:892-899.$
- Kim S, Aksak B, Sitti M. Enhanced friction of elastomer microfiber adhesives with spatulate tips. Appl Phys Lett 2007;91:221913.
- Tamelier J, Chary S, Turner K, Yu J, Das S, Israelachvili J. Millimeter size patch behavior of gecko-inspired reversible adhesive. Sensors IEEE 2011; 1819–1822.

- Vellayappan MV, Jaganathan SK, Supriyanto E. Review: unraveling the less explored flocking technology for tissue engineering scaffolds. RSC Adv 2015:5:73225-73240.
- Cipitria A, Skelton A, Dargaville TR, Dalton PD, Hutmacher DW. Design, fabrication and characterization of PCL electrospun scaffolds—a review. J Mater Chem 2011;21:9419–9453.
- Varagnolo S, Raccanello F, Pierno M, et al. Highly sticky surfaces made by electrospun polymer nanofibers. RSC Adv 2017;7:5836–5842.
- Coimbra P, Freitas JP, Goncalves T, Gil MH, Figueiredo M. Preparation of gentamicin sulfate eluting fiber mats by emulsion and by suspension electrospinning. Korean J Couns Psychother 2019;94:86–93.
- Corradetti B. The Immune Response to Implanted Materials and Devices. Switzerland: Springer International Publishing; 2017.
- Wang W, Junior JRP, PRL N, et al. Engineered 3D printed poly (e-caprolactone)/graphene scaffolds for bone tissue engineering. Mater Sci Eng C 2019;100:759–770.
- Chou SF, Woodrow KA. Relationships between mechanical properties and drug release from electrospun fibers of PCL and PLGA blends. J Mech Behav Biomed Mater 2017;65:724–733.
- Rychter M, Milanowski B, Grzeskowiak BF, et al. Cilostazol-loaded electrospun three-dimensional systems for potential cardiovascular application: effect of fibers hydrophilization on drug release, and cytocompatibility. J Colloid Interface Sci 2019;536:310–327.
- Jang CH, Cho YB, Jang YS, Kim MS, Kim GH. Antibacterial effect of electrospun polycaprolactone/polyethylene oxide/vancomycin nanofiber mat for prevention of periprosthetic infection and biofilm formation. Int J Pediatr Otorhinolaryngol 2015;79:1299–1305.
- Rasti Boroojen F, Mashayekhan S, Abbaszadeh HA. The controlled release
 of dexamethasone sodium phosphate from bioactive electrospun PCL/
 gelatin Nanofiber scaffold. Iran J Pharm Res 2019;18:111-124.
- Da Silva GR, Lima TH, Fernandes-Cunha GM, et al. Ocular biocompatibility of dexamethasone acetate loaded poly(varepsilon-caprolactone) nanofibers. Eur J Pharm Biopharm 2019;142:20–30.
- 31. Wang Y, Ma B, Yin A, et al. Polycaprolactone vascular graft with epigallocatechin gallate embedded sandwiched layer-by-layer functionalization for enhanced antithrombogenicity and anti-inflammation. J Control Release 2020;320:226–238.
- 32. Machado BR, Roberto SB, Bonafé EG, et al. Chitosan imparts better biological properties for poly (ε -caprolactone) electrospun membranes than dexamethasone. *J Braz Chem Soc* 2019;30:1741–1750.
- Walther A, Hoyer B, Springer A, et al. Novel textile scaffolds generated by flock technology for tissue engineering of bone and cartilage. *Materials* 2012;5:540–557.
- Gossla E, Tonndorf R, Bernhardt A, et al. Electrostatic flocking of chitosan fibres leads to highly porous, elastic and fully biodegradable anisotropic scaffolds. Acta Biomater 2016;44:267–276.
- Davis NF, Mulvihill JJ, Mulay S, Cunnane EM, Bolton DM, Walsh MT. Urinary bladder vs gastrointestinal tissue: a comparative study of their biomechanical properties for urinary tract reconstruction. *Urology* 2018;113: 235–240.
- Özgür E, Bereli N, Türkmen D, Ünal S, Denizli A. PHEMA cryogel for in vitro removal of anti-dsDNA antibodies from SLE plasma. *Mater Sci Eng C* 2011:31:915–920.

- Mine Y, Mitsui H, Oshima Y, Noishiki Y, Nakai M, Sano S. Suture retention strength of expanded polytetrafluoroethylene (ePTFE) graft. Acta Med Okayama 2010;64:121–128.
- Meng X, Wang X, Jiang Y, Zhang B, Li K, Li Q. Suture retention strength of P (LLA-CL) tissue-engineered vascular grafts. RSC Adv 2019;9: 21258–21264.
- McKenna KA, Hinds MT, Sarao RC, et al. Mechanical property characterization of electrospun recombinant human tropoelastin for vascular graft biomaterials. Acta Biomater 2012;8:225–233.
- Pensalfini M, Meneghello S, Lintas V, Bircher K, Ehret AE, Mazza E. The suture retention test, revisited and revised. J Mech Behav Biomed Mater 2018;77:711-717.
- Parlato M, Reichert S, Barney N, Murphy WL. Poly (ethylene glycol) hydrogels with adaptable mechanical and degradation properties for use in biomedical applications. *Macromol Biosci* 2014;14:687–698.
- Davis RJ, Hillel AT. Inflammatory pathways in the pathogenesis of iatrogenic laryngotracheal stenosis: what do we know? Transl Cancer Res 2020-9:2108-2116
- Tan F, Zhu Y, Ma Z, Al-Rubeai M. Recent advances in the implant-based drug delivery in otorhinolaryngology. Acta Biomater 2020;108:46–55.
 Wierzbicka M, Tokarski M, Puszczewicz M, Szyfter W. The efficacy of sub-
- Wierzbicka M, Tokarski M, Puszczewicz M, Szyfter W. The efficacy of submucosal corticosteroid injection and dilatation in subglottic stenosis of different aetiology. J Laryngol Otol 2016;130:674–679.
- Hoffman MR, Coughlin AR, Dailey SH. Serial office-based steroid injections for treatment of idiopathic subglottic stenosis. Laryngoscope 2017;127: 2475-2481
- 46. Franco RA Jr, Husain I, Reder L, Paddle P. Awake serial intralesional steroid injections without surgery as a novel targeted treatment for idiopathic subglottic stenosis. *Laryngoscope* 2018;128:610–617.
- Fussey JM, Borsetto D, Pelucchi S, Ciorba A. Surgical management of acquired anterior glottic web: a systematic review. J Laryngol Otol 2019; 1–8. https://doi.org/10.1017/S0022215119001920.
- Zapater E, Oishi N, Arribas M, Hernandez R, Lopez I, Basterra J. Use of bovine pericardium for the treatment of anterior iatrogenic glottic web. Laryngoscope 2019;129:2121–2124.
- Yilmaz T. Surgical treatment of glottic web using butterfly mucosal flap technique: experience on 12 patients. Laryngoscope 2019;129:1423–1427.
- Mahdavi A, Ferreira L, Sundback C, et al. A biodegradable and biocompatible gecko-inspired tissue adhesive. Proc Natl Acad Sci 2008;105: 2307–2312.
- 51. Autumn K. Properties, principles, and parameters of the gecko adhesive system. In: Smith AM, Callow JA, eds. Biological Adhesives. Berlin, Heidelberg: Springer Berlin Heidelberg; 2006:225–256.
 52. Pendekal MS, Tegginamat PK. Formulation and evaluation of a bioadhesive
- Pendekal MS, Tegginamat PK. Formulation and evaluation of a bioadhesive patch for buccal delivery of tizanidine. *Acta Pharm Sin B* 2012;2:318–324.
 Shaikh R, Raj Singh TR, Garland MJ, Woolfson AD, Donnelly RF.
- Shaikh R, Raj Singh TR, Garland MJ, Woolfson AD, Donnelly RF. Mucoadhesive drug delivery systems. J Pharm Bioallied Sci 2011;3: 89-100
- Beule AG, Scharf C, Biebler KE, et al. Effects of topically applied dexamethasone on mucosal wound healing using a drug-releasing stent. *Laryngo-scope* 2008;118:2073–2077.
- 55. Boazak EM, Auguste DT. Trachea mechanics for tissue engineering design. $ACS\ Biomater\ Sci\ Eng\ 2018;4:1272-1284.$